Partial Orientation of Oxidized and Reduced Cytochrome b_5 at High Magnetic Fields: Magnetic Susceptibility Anisotropy Contributions and Consequences for Protein Solution Structure Determination

Lucia Banci,[†] Ivano Bertini,*[,†] J. Gaspard Huber,[‡] Claudio Luchinat,[‡] and Antonio Rosato[†]

Contribution from the Department of Chemistry, University of Florence, Florence, Italy, and Department of Soil Science and Plant Nutrition, University of Florence, Florence, Italy

Received May 22, 1998. Revised Manuscript Received September 24, 1998

Abstract: The backbone $^{15}N-^{1}H$ ^{1}J values have been measured for oxidized and reduced cytochrome b_5 at 500 and 800 MHz. Their field dependence, due to increasing partial orientation of the molecule in solution at high magnetic fields, provides structural constraints relative to the orientation of the NH bond vector with respect to the principal directions of the molecular susceptibility tensor. The constraints have been used in a distance geometry algorithm together with the NOE constraints and with or without pseudocontact shifts constraints. The three sets of constraints are found to be consistent with one another, and their relative contribution to the definition of the structure depends on the number of constraints and their assigned weight. The orientation-dependent $^{15}N-^{1}H$ ^{1}J values provide the principal directions and anisotropies of the molecular or overall magnetic susceptibility tensor, χ^{mol}. The χ^{mol} parameters obtained for the oxidized form differ from those for the diamagnetic reduced form essentially by the magnetic susceptibility of the paramagnetic ion, whose anisotropy is responsible for the occurrence of pseudocontact shifts. The χ^{mol} tensor of the paramagnetic form displays a sizable rhombic anisotropy, thus permitting the full assessment of the orientation of individual amide vectors in the molecular axes frame.

Introduction

All molecules with a nonzero molecular magnetic susceptibility (χ^{mol}) anisotropy adopt preferred orientations in an external magnetic field. This is due to the fact that different orientations of the molecules result in different induced magnetic moments, which then have different energies of interaction with the magnetic field. The orientation of the molecules in solution obeys a Boltzmann distribution, the degree of alignment being proportional to B_0^2.[1] The high magnetic fields now available induce an alignment sufficient to give rise to effects detectable through NMR spectroscopy.[2] The partial orientation of the molecules causes incomplete rotational averaging of dipolar[3] and quadrupolar[4] couplings, which produce additional or new splittings in the high-resolution NMR spectra. Such effects have been indeed observed in diamagnetic[1,2,4−9] and in paramagnetic[3,10] small molecules. The chemical shifts are also reported to be dependent on the magnetic ordering in solution, again for both diamagnetic[11] and paramagnetic[12] molecules.

The noncompletely averaged couplings, or residual dipolar couplings (rdc) constitute a source of structural information which may have a great impact on the protocols used for solution structure determination by NMR.[13−16] The key feature of these potential constraints is that they can define long-range ordering in a molecule. This potentiality would be quite helpful for solution structure determination, which is otherwise mostly based on the measurement of short (<5−6 Å) interproton distances. A study on the use of rdc for the structural refinement of a DNA−protein complex has been recently published, where these constraints proved useful in determining the correct orientation of a protein loop and in improving the overall quality of the structure.[15] For this purpose, a routine for the use of rdc constraints was implemented in the X-PLOR program.[17]

As rdc are more easily measured the larger the molecular magnetic susceptibility anisotropy, the investigation of molecules containing paramagnetic metal ions is particularly promising.[12,13]

* Corresponding author: (fax) +39 055 2757555; (tel) +39 055 2757549; (e-mail) bertini@lrm.fi.cnr.it.

† Department of Chemistry.

‡ Department of Soil Science and Plant Nutrition.

(1) van Zijl, P. C. M.; Ruessink, B. H.; Bulthuis, J.; Maclean, C. *Acc. Chem. Res.* **1984**, *17*, 172−180.

(2) Bothner-By, A. A. In *Encyclopedia of Nuclear Magnetic Resonance*; Grant, D. M., Harris, R. K. Eds.; John Wiley and Sons: Chichester, U.K., 1996; pp 2932−2938.

(3) Bothner-By, A. A.; Domaille, J. P.; Gayathri, C. *J. Am. Chem. Soc.* **1981**, *103*, 5602−5603.

(4) Bothner-By, A. A.; Gayathri, C.; van Zijl, P. C. M.; Maclean, C.; Lai, J.; Smith, K. M. *Magn. Reson. Chem.* **1985**, *23*, 935−938.

(5) Lohman, J. A. B.; Maclean, C. *Chem. Phys.* **1978**, *35*, 269−274.

(6) Lohman, J. A. B.; Maclean, C. *Chem. Phys. Lett.* **1978**, *58*, 483−486.

(7) Lohman, J. A. B.; Maclean, C. *J. Magn. Reson.* **1981**, *42*, 5−13.

(8) Bothner-By, A. A.; Gayathri, C.; van Zijl, P. C. M.; Maclean, C. *J. Magn. Reson.* **1984**, *56*, 456−462.

(9) Gayathri, C.; Bothner-By, A. A.; van Zijl, P. C. M.; Maclean, C. *Chem. Phys. Lett.* **1982**, *87*, 192−196.

(10) Domaille, J. P. *J. Am. Chem. Soc.* **1980**, *102*, 5392−5393.

(11) Ottiger, M.; Tjandra, N.; Bax, A. *J. Am. Chem. Soc.* **1997**, *119*, 9825−9830.

(12) Bertini, I.; Felli, I. C.; Luchinat, C. *J. Magn. Reson.* **1998**, *134*, 360−364.

(13) Tolman, J. R.; Flanagan, J. M.; Kennedy, M. A.; Prestegard, J. H. *Proc. Natl. Acad. Sci. U.S.A.* **1995**, *92*, 9279−9283.

(14) Tjandra, N.; Grzesiek, S.; Bax, A. *J. Am. Chem. Soc.* **1996**, *118*, 6264−6272.

(15) Tjandra, N.; Omichinski, J. G.; Gronenborn, A. M.; Clore, G. M.; Bax, A. *Nature Struct. Biol.* **1997**, *4*, 732−738.

(16) Clore, G. M.; Gronenborn, A. M.; Tjandra, N. *J. Magn. Reson.* **1998**, *131*, 159−162.

(17) Brunger, A. T. *X-PLOR Manual Version 3.1. A System for X-ray Cristallography and NMR*; Yale University Press: New Haven, CT, 1992.

10.1021/ja981791w CCC: $15.00
Published on Web 11/25/1998

A metal ion displaying magnetic susceptibility anisotropy would also induce pseudocontact shifts (pcs), which are due to the dipolar interaction between the nuclear magnetic moment and the orientation-dependent electron magnetic moment.[18,19] In most favorable cases (i.e., when the magnetic susceptibility anisotropy of the metal is large), pcs can be accurately measured at more than 15 Å from the metal ion. Pcs provide additional structural constraints, already used for solution structure determination.[20,21] Therefore, the paramagnetic susceptibility anisotropy (χ^{para}) is at the same time the direct source of pcs and a major contributor to the molecular susceptibility anisotropy and thus to rdc.

In the present work, rdc are measured for a paramagnetic heme-containing protein, namely oxidized cytochrome b_5 (cyt b_5) from rat, and for the diamagnetic reduced species. The rdc constraints are used for solution structure refinement, and the relative importance of pcs and rdc constraints with respect to the precision/accuracy of the calculated structure is discussed. It is also shown that it is possible to use both classes of constraints simultaneously with satisfactory results. The molecular magnetic susceptibility anisotropies of the oxidized and reduced species are obtained from the rdc values and the final structure. Their difference is accounted for by the magnetic susceptibility anisotropy of the paramagnetic metal ion, which is responsible for pcs, and therefore independently measured. In addition, the approach to the use of rdc constraints for solution structure determination described in this work constitutes a straightforward computational strategy for dealing with rhombic magnetic susceptibility tensors.

Materials and Methods

Sample Preparation. Recombinant rat microsomal cytochrome b_5 was isolated as previously described.[22] About 9 mg of protein was exchanged with a 10 mM potassium phosphate buffer at pH 7.0 and then concentrated through ultracentrifugation to a volume of 400 μL to reach a final concentration of ~2 mM in protein. The pH was adjusted to 7.0 by addition of small volumes of concentrated HCl and NaOH solutions. D_2O (50 μL) was added for field-frequency lock.

For the reduced form, a solution ~1 mM in protein was prepared as above and carefully purged with argon. Solid sodium dithionite was then added as the reducing agent.

NMR Spectroscopy. NMR experiments were carried out at 25 °C on AVANCE 800 and DRX 500 spectrometers. The temperature was calibrated using the difference of the chemical shift of methylene and methyl peaks of an ethanol sample in water, after 64 dummy cycles of the sequence used for the measurement of $^{15}N-^{1}H$ ^{1}J (see below).

A series of 10 spectra was recorded using a $^{15}N-^{1}H$ ^{1}J-modulated HSQC sequence[14] with dephasing delays, 2Δ, including a pulsed field gradient, of 44.0, 45.8, 47.6, 49.4, 51.2, 54.8, 56.6, 58.4, 60.2, and 62.0 ms. The intensities of cross-peaks are then given by[14]

$$I(2\Delta) = A \cos(2\pi J_{NH}\Delta) \exp(-(2\Delta/T_2^*)) \quad (1)$$

where $1/T_2^*$ is the effective decay rate of the ^{15}N magnetization in the *xy* plane, originating from both transverse relaxation and unresolved long-range $^{15}N-^{1}H$ ^{1}J. *A* is the intensity of the cross-peak when Δ is null.

As previously suggested,[14] 2Δ values should be chosen as two sets of symmetric values around $(2n + 1)/2J$, where *n* is an integer, to take into account effects of 180° ^{15}N pulse imperfections and to optimize the accuracy of the measurement of *J*. The best value of *n*, which depends on the value of T_2^*, was chosen after measuring T_2^* of some cross-peaks from the $^{1}J_{HN}$-modulated HSQC spectra acquired with Δ delays of 5.3, 10.6, and 21.2 ms. These delays correspond to $1/2J$, $1/J$, and $2/J$ and yield almost completely refocused intensity for all NH moieties. Therefore, for these Δ delays the HSQC cross-peak intensities are only dependent on the transverse relaxation of ^{15}N spins. An average T_2^* value of 40 ms was found in both oxidized and reduced forms of the protein; *n* was thus set as 4 and 5.

At 800 MHz, two sets of experiments of 32 scans each were performed on the oxidized form of the protein, and one on the reduced form. At 500 MHz, for both forms, one set of experiments was performed with 48 scans and another with 16 scans. The total experiment time for the set constituted by 32 scans was ~33 h at 800 MHz. The series of experiments with 48 scans was recorded in ~50 h. The 180° ^{15}N pulse ranged from 60 to 70 μs on both DRX 500 and AVANCE 800 spectrometers.

After multiplication by a 90° shifted sine-bell, the 2D spectra were baseline corrected. Cross-peaks were integrated using the standard Bruker software. Rectangular boxes at the noise level were used to define the integration region, except for overlapping cross-peaks, for which smaller boxes were chosen in order to minimize the contribution from the unwanted peak.

Structure Calculations. Structure calculations were run on a IBM SP02 parallel computer using the simulated annealing, torsion angle dynamics program DYANA.[23] Pseudocontact shifts were introduced in the calculations of the structure of the oxidized form by following the previously outlined procedure[24] through a modified version of DYANA, which is referred to as PSEUDYANA.[25]

All constraints other than rdc were taken from previous works[24,26] without modification. This corresponded to 1203 meaningful NOEs for the reduced form[26] and to 1372 meaningful NOEs and 235 pseudocontact shifts for the oxidized form.[24]

Determination of the Molecular Magnetic Susceptibility Anisotropy. The rdc values are given by[1] (in SI units)

$$\text{rdc (Hz)} = -\frac{1}{4\pi}\frac{B_0^2}{15\,kT}\frac{\gamma_H\gamma_N h}{4\pi^2 r_{HN}^3}\left[\Delta\chi_{ax}(3\cos^2\theta - 1) + \frac{3}{2}\Delta\chi_{rh}(\sin^2\theta\cos 2\phi)\right] \quad (2)$$

where $\Delta\chi_{ax}$ and $\Delta\chi_{rh}$ are the axial and rhombic anisotropies of the χ^{mol} tensor and θ and ϕ are polar coordinates describing the orientation of the N−H bond vector in the axis system of the χ^{mol} tensor. The structural constraints actually used are the *differences* between rdc (which will be referred to as Δrdc) values measured at two different fields (18.7 and 11.7 T in this work), which are obtained from eq 2, by replacing B_0^2 with ΔB_0^2.

The magnetic susceptibility tensor parameters are obtained by best fitting the experimental Δrdc values to eq 2, by using an input structural model. The adjustable parameters are the $\Delta\chi_{ax}$ and $\Delta\chi_{rh}$ values and the three independent direction cosines needed to define the orientation of the χ^{mol} tensor with respect to the laboratory frame. When dealing with a family of conformers (e.g., obtained from DYANA calculations), all conformers are superimposed by best fitting the coordinates of the backbone heavy atoms of the well-defined regions of the protein, and the parameters for the average χ^{mol} tensor are determined. The quantity which is minimized is

(18) McConnell, H. M.; Robertson, R. E. *J. Chem. Phys.* **1958**, *29*, 1361−1365.
(19) Kurlanol, R. J.; McGarvey, B. R. *J. Magn. Reson.* **1970**, *2*, 286−301.
(20) Bertini, I.; Luchinat, C.; Rosato, A. *Prog. Biophys. Mol. Biol.* **1996**, *66*, 43−80.
(21) Bertini, I.; Rosato, A. In *Molecular Modeling and Dynamics of Bioinorganic Systems*; Banci, L., Comba, P., Eds.; Kluwer Academic Publishers: Dordrecht, The Netherlands, 1997; pp 1−19.
(22) von Bodman, S. B.; Schulder, M. A.; Jollie, D. R.; Sligar, S. G. *Proc. Natl. Acad. Sci. U.S.A.* **1986**, *83*, 9443−9447.
(23) Güntert, P.; Mumenthaler, C.; Wüthrich, K. *J. Mol. Biol.* **1997**, *273*, 283−298.
(24) Arnesano, F.; Banci, L.; Bertini, I.; Felli, I. C. *Biochemistry* **1998**, *37*, 173−184.
(25) Banci, L.; Bertini, I.; Cremonini, M. A.; Gori Savellini, G.; Güntert, P.; Luchinat, C.; Wüthrich, K. *J. Biomol. NMR*, in press.
(26) Banci, L.; Bertini, I.; Ferroni, F.; Rosato, A. *Eur. J. Biochem.* **1997**, *249*, 270−279.

$$U = \sum_{s=1}^{N}\sum_{i=1}^{D} w_i[\Theta(|\Delta\mathrm{rdc}^{i,s}_{\mathrm{calc}} - \Delta\mathrm{rdc}^{i}_{\mathrm{exp}}|, T_i)]^2 \quad (3)$$

where

$$\Theta(|\Delta\mathrm{rdc}^{i,s}_{\mathrm{calc}} - \Delta\mathrm{rdc}^{i}_{\mathrm{exp}}|, T_i) = \begin{cases} 0 & \text{if } |\Delta\mathrm{rdc}^{i,s}_{\mathrm{calc}} - \Delta\mathrm{rdc}^{i}_{\mathrm{exp}}| < T_i \\ \text{else} & |\Delta\mathrm{rdc}^{i,s}_{\mathrm{calc}} - \Delta\mathrm{rdc}^{i}_{\mathrm{exp}}| - T_i \end{cases}$$

The first summation runs on the N conformers of the family and the second one on the D experimental Δrdc values. w_i and T_i (both ≥ 0) are respectively the weight and the tolerance assigned to the ith experimental value. In the present work, all weights were taken equal. The tolerance values were different for the oxidized and reduced species, but within one species they were all taken equal to the mean value of the experimental error on the Δrdc's (0.2 Hz for the reduced species, and 0.1 Hz for the oxidized). The above approach is analogous to that already developed by us for the determination of the paramagnetic susceptibility tensor from pseudocontact shifts.[20,24,27,28]

Introduction of Residual Dipolar Coupling Constraints in Structure Calculations. We have developed a new routine to include Δrdc constraints in structure calculations. This routine was implemented in the PSEUDYANA module of the program DYANA. In the present system, the contribution to the residual dipolar coupling due to the rhombic anisotropy was not negligible, and thus a complete treatment was necessary. An analysis of rdc data in a rhombic system has been recently reported by Clore et al.[16]

A new term (V_{rdc}) has been added to the target function (V) of PSEUDYANA. The new term is defined as

$$V_{\mathrm{rdc}} = \omega_{\mathrm{rdc}} \sum_{i=1}^{D} w_i[\Theta(|\Delta\mathrm{rdc}^{i}_{\mathrm{calc}} - \Delta\mathrm{rdc}^{i}_{\mathrm{exp}}|, T_i)]^2 \quad (4)$$

where

$$\Theta(|\Delta\mathrm{rdc}^{i}_{\mathrm{calc}} - \Delta\mathrm{rdc}^{i}_{\mathrm{exp}}|, T_i) = \begin{cases} 0 & \text{if } |\Delta\mathrm{rdc}^{i}_{\mathrm{calc}} - \Delta\mathrm{rdc}^{i}_{\mathrm{exp}}| < T_i \\ \text{else} & |\Delta\mathrm{rdc}^{i}_{\mathrm{calc}} - \Delta\mathrm{rdc}^{i}_{\mathrm{exp}}| - T_i \end{cases}$$

w_i is the relative weight of the ith constraint and ω_{rdc} is the weighting factor of the Δrdc constraints, which is used to scale the contribution to the target function from this class of constraints with respect to the contribution from the other constraints (NOEs, dihedral angle constraints and pseudocontact shifts in this case). All other symbols have been already defined (see comments to eq 3). As already done for the PSEUDYANA program,[25] the input parameters relative to the χ^{mol} tensor for the structure calculations are limited to the $\Delta\chi_{\mathrm{ax}}$ and $\Delta\chi_{\mathrm{rh}}$ values, as the orientation of the tensor in the molecular frame is adjusted by the program. This was accomplished by imposing that the χ^{mol} tensor axis system coincided with the internal axis system used by DYANA and letting the whole protein orient with respect to it in order to minimize the target function. For reduced cyt b_5, the following calculation parameters were used: all w_i values were equal to 1, $\omega_{\mathrm{rdc}} = 0.4$ and all T_i values were equal to 0.2. In the case of oxidized cyt b_5, the above values were $w_i = 1$, $\omega_{\mathrm{rdc}} = 0.4$, and $T_i = 0.1$. The lower value of T_i in the second case reflected the smaller average error obtained in the Δrdc measurements (see Supporting Information). The new family of conformers was used as input structural model to re-estimate the tensor parameters, as described in the preceding section, for a new refinement step.

Results

Determination of rdc Contributions to $^1J_{\mathrm{HN}}$ Values. NMR spectral assignment had been previously performed in our laboratory[24,26] and found to be in good agreement with earlier ones.[29−31] The protein exists in a major form A and in a minor form B, differing by a 180° rotation of the heme about the α−γ meso axis.[32,33] Cross-peaks corresponding to form B were not taken into consideration: only cross-peaks arising from form A and cross-peaks unresolved for both forms were used. A total of 63 and 56 ^{1}H−^{15}N ^1J couplings were measured at both fields for the oxidized and reduced forms, respectively. Their values are given in the Supporting Information, Tables 1 and 2. Values relative to Leu 94 were not used in calculations due to the high mobility of this residue.

After the addition of $2/\pi$ times the duration of the 180° ^{15}N pulse to the 2Δ values, to account for the dephasing angle during the 180° ^{15}N pulse,[14] peak volumes were fitted as a function of 2Δ with the three parameters A, J_{NH}, and T_2* of eq 1. For the oxidized form, the pairwise root-mean-square difference between the results of the two sets of experiments recorded at the same magnetic field was 0.07 Hz at both magnetic fields. These values were comparable to those previously reported for other systems.[14,34] Nevertheless, one should keep in mind that this is an estimate of the random error and that a systematic error between the experiments at 800 and 500 MHz may also be present. For the reduced form, the pairwise root-mean-square difference was 0.14 Hz at 500 MHz (see Supporting Information). The larger error in the values observed for the reduced form could be partly due to the lower concentration of the sample.

The difference between the values of $^1J_{\mathrm{HN}}$ measured at two different fields is determined by two magnetic field dependent effects: rdc and dynamic frequency shift (δ_{DFS}). To use Δrdc's as constraints for solution structure determination, it is necessary to introduce a correction for the contribution arising from δ_{DFS}.[14] The latter depends on the rotational regime of the molecule.[14,35] The relative values of the principal components of the inertia tensor of cyt b_5 are 1:0.94:0.67. The rotational diffusion tensor (**D**) of cyt b_5 is thus expected to be nonisotropic, but essentially axially symmetric. In this case, the value of the δ_{DFS} depends on the relative orientations of the diffusion and CSA tensors and on the orientation of the NH bond vector with respect to the two tensors.[14,35] Each NH moiety will thus have a different value of δ_{DFS}. The pertinent equation is

$$\delta_{\mathrm{DFS}}(B_0) = \frac{S^2}{40\pi^3} h(\sigma_{\parallel} - \sigma_{\perp}) \frac{\gamma_{\mathrm{N}}\gamma_{\mathrm{H}}}{r_{\mathrm{NH}}^3} \left\{ \frac{(3\cos^2\eta_{\mathrm{D}} - 1)(3\cos^2\eta_{\mathrm{C}} - 1)}{1 + (\gamma_{\mathrm{N}}B_0\tau_1)^{-2}} + \frac{12\cos\eta_{\mathrm{D}}\cos\eta_{\mathrm{C}}\sin\eta_{\mathrm{D}}\sin\eta_{\mathrm{C}}\cos(\phi_{\mathrm{D}} - \phi_{\mathrm{C}})}{1 + (\gamma_{\mathrm{N}}B_0\tau_2)^{-2}} + \frac{3\sin^2\eta_{\mathrm{D}}\sin^2\eta_{\mathrm{C}}\cos(2\phi_{\mathrm{D}} - 2\phi_{\mathrm{C}})}{1 + (\gamma_{\mathrm{N}}B_0\tau_3)^{-2}} \right\} \quad (5)$$

where $\tau_1 = (6D_{\perp})^{-1}$, $\tau_2 = (D_{\parallel} + 5D_{\perp})^{-1}$, and $\tau_3 = (4D_{\parallel} +$

(27) Bentrop, D.; Bertini, I.; Cremonini, M. A.; Forsén, S.; Luchinat, C.; Malmendal, A. *Biochemistry* **1997**, *36*, 11605−11618.
(28) Banci, L.; Bertini, I.; Gray, H. B.; Luchinat, C.; Reddig, T.; Rosato, A.; Turano, P. *Biochemistry* **1997**, *36*, 9867−9877.
(29) Guiles, R. D.; Basus, V. J.; Kuntz, I. D.; Waskell, L. *Biochemistry* **1992**, *31*, 11365−11375.
(30) Guiles, R. D.; Basus, V. J.; Sarma, S.; Malpure, S.; Fox, K. M.; Kuntz, I. D.; Waskell, L. *Biochemistry* **1993**, *32*, 8329−8340.
(31) Sarma, S.; DiGate, R. J.; Banville, D.; Guiles, R. D. *J. Biomol. NMR* **1996**, *8*, 171−183.
(32) Keller, R. M.; Wüthrich, K. *Biochim. Biophys. Acta* **1980**, *621*, 204−217.
(33) McLachlan, S. J.; La Mar, G. N.; Burns, P. D.; Smith, K. D.; Langry, K. C. *Biochim. Biophys. Acta* **1986**, *874*, 274−284.
(34) Tolman, J. R.; Prestegard, J. H. *J. Magn. Reson. Ser. B* **1996**, *112*, 245−252.
(35) Werbelow, L. In *Encyclopedia of Nuclear Magnetic Resonance*; Grant, D. M., Harris, R. K., Eds.; John Wiley & Sons: Chichester, U.K., 1996; pp 1776−1783.

Table 1. Parameters Characterizing the χ^{mol} and the χ^{dia} Tensors of the Oxidized and the Reduced Protein, Respectively, and the χ^{para} Tensor

	tensor			
	χ^{dia} [a,b]	χ^{para} [a,c]	χ^{mol} [a,d]	calcd χ^{mol} tensor[e]
$\Delta\chi_{ax}$ ($/10^{-32}$ m^3)	-0.8 ± 0.1	2.8 ± 0.1	2.20 ± 0.05	2.1 ± 0.2
$\Delta\chi_{rh}$ ($/10^{-32}$ m^3)	0.1 ± 0.3	-1.1 ± 0.2	-1.34 ± 0.04	-1.0 ± 0.5
deviation of the *z* axis from the normal to the heme plane (deg)	15 ± 12	2 ± 3	3 ± 14	11 ± 12
deviation of the *x* axis from the $\alpha-\gamma$ meso axis (deg)	-4 ± 43	8 ± 6	5 ± 6	2 ± 22

[a] The reported error on the $\Delta\chi$ parameters is the standard deviation from the mean of the 20 values obtained by fitting each conformer individually. The uncertainty on the angles was taken equal to the largest deviation from the optimal solution yielding a sum of the squared differences between calculated and experimental Δrdc (or pcs) values smaller than twice the sum evaluated for the optimal solution itself. [b] Obtained by fitting the 55 Δrdc's to eq 2 using as input the refined DYANA family. [c] Obtained by fitting the 235 pseudocontact shifts to the refined PSEUDYANA family. The present values are calculated for comparison purposes and are slightly different from those already reported, calculated on an energy-minimized family.[24] [d] Obtained by fitting the 62 Δrdc's to eq 2 using as input the refined PSEUDYANA family. [e] Obtained from the tensorial sum of the experimental χ^{dia} and the χ^{para} tensors.

Table 2. Statistical Analysis of Structure Calculations for Reduced Cyt b_5 Run with NOE Only and with NOE and Δrdc[a]

	only NOE	NOE and Δrdc
backbone RMSD[b] (residues 4−89) (Å)	0.76 ± 0.11	0.74 ± 0.14
NOE and van der Waals target function (Å^2)	0.94 ± 0.20	0.95 ± 0.18
total target function (Å^2)	0.94 ± 0.20	1.21 ± 0.18
av violation per NOE constraint (Å)	0.0041 ± 0.0005	0.0040 ± 0.0005
av no. of violations >0.05 Å per structure	36 ± 7	33 ± 7
av no. of violations >0.2 Å per structure	1 ± 1	0 ± 1
largest residual NOE violation[c]	0.42 Å	0.41 Å
av deviation per Δrdc constraint (Hz)[d]	0.07 ± 0.01	0.025 ± 0.006
av no. of Δrdc violations	38.4 ± 1.8	29.5 ± 2.0

[a] All values are averaged over the best 20 conformers, unless otherwise indicated. [b] These values have been recalculated by using the present DYANA structures, as discussed in the experimental part, for comparison purposes. [c] Largest violation among all 20 conformers. [d] Average deviation between experimental and calculated values.

$2D_\perp)^{-1}$. The angle between the unique axes of the dipolar and diffusion tensor is η_D, and that between the axially symmetric CSA tensor and the diffusion tensor is η_C. The difference $\phi_D - \phi_C$ refers to the angle between projections of the unique axes of the dipolar and CSA tensors on the plane perpendicular to the unique axis of the diffusion tensor. h is Planck's constant, γ_N and γ_H are the gyromagnetic ratios for ^{15}N and ^{1}H, r_{NH} is the N−H internuclear distance (1.02 Å), B_0 is the external magnetic field, and S^2 is the generalized order parameter. However, we are only interested in the difference between the δ_{DFS} values at the two fields at which the measurements were done (vide infra). In the present case, by assuming an angle of 24° between the unique axes of the dipolar tensor of the ^{1}H−^{15}N vector and the principal axis of ^{15}N CSA tensor,[36] a difference between parallel and orthogonal chemical shift for the CSA tensor of ^{15}N of −160 ppm, and a uniform S^2 value of 0.85,[37] these differences were found to be in the 0.075−0.085-Hz range. Therefore, although the above parameters used to calculate the δ_{DFS} are only reasonable estimates rather than experimental values, only a minor error is introduced in the estimate of Δrdc.

The Δrdc values were calculated by the following relation

$$\Delta\text{rdc} = -[(J_{800\text{MHz}} - J_{500\text{MHz}}) + (\delta_{\text{DFS800MHz}} - \delta_{\text{DFS500MHz}})] \quad (6)$$

The negative sign in front of eq 6 is because the ^{1}H−^{15}N scalar coupling is negative.[13] However, it is customary to report $^1J_{HN}$ values as positive numbers. Thus, in eq 6, $J_{800\ MHz}$ and $J_{500\ MHz}$ are positive numbers, and the δ_{DFS} values are obtained from eq 5. Δrdc values are reported in the Supporting Information.

Structure Calculation Results. Initial values for the χ^{mol} tensor parameters for reduced and oxidized cytochrome b_5 were obtained by fitting the Δrdc values using as input models, respectively, the DYANA and PSEUDYANA families previously obtained without Δrdc constraints.[24,26] These values are needed for the solution structure calculations (see Methods and Materials). For oxidized cyt b_5, the initial values were $\Delta\chi_{ax} = 1.4 \times 10^{-32}$ m^3, $\Delta\chi_{rh} = -0.6 \times 10^{-32}$ m^3. For reduced cyt b_5, the corresponding values were $\Delta\chi_{ax} = -0.6 \times 10^{-32}$ m^3, $\Delta\chi_{rh} = 0.2 \times 10^{-32}$ m^3.

When the new Δrdc constraints were used together with all the other constraints in structural calculations from the beginning of simulated annealing calculations (using the standard DYANA protocol[23]), the program failed to yield a family of conformers satisfying all the experimental constraints. Different annealing schemes were tried out, none of which lead to satisfactory results. A different approach was therefore followed. After generating a family of 250 conformers without using the new constraints, the 100 conformers with the lower target function were subjected to conjugate gradient minimization using all the previous constraints and the Δrdc constraints simultaneously. This protocol, available in DYANA, is essentially a distance geometry protocol which minimizes the target function by varying the dihedral angles. The 20 minimized conformers with lowest *total* target function were collected to form the final family of structures. This family was then used as the input structural model for a new determination of the magnetic susceptibility tensor parameters, and the resulting $\Delta\chi_{ax}$ and $\Delta\chi_{rh}$ values were then used for a new minimization of the 100 conformers obtained without dipolar coupling constraints. This procedure was iterated until the tensor parameters reached convergence, and the last family of minimized conformers was employed for all subsequent analyses. The output is substantially of the same quality, in terms of RMSD, of the structures obtained with only NOEs and consistent (see the target function values in Tables 2 and 3) with the new Δrdc constraints (Tables

(36) Hiyama, Y.; Niu, C. H.; Silverston, J. V.; Bavoso, A.; Torchia, D. A. *J. Am. Chem. Soc.* **1988**, *110*, 2378−2383.
(37) Dangi, B.; Sarma, S.; Yan, C.; Banville, D. L.; Guiles, R. D. *Biochemistry* **1998**, *37*, 8289−8302.

Table 3. Statistical Analysis of Structure Calculations for Oxidized Cyt b_5 Run with NOE Only, with NOE and Δrdc, with NOE and pcs, and with the Sets of Constraint Together[a]

	only NOE	NOE and pcs	NOE and Δrdc	NOE, pcs, and Δrdc
backbone RMSD[b] (residues 4−84) (Å)	0.58 ± 0.11	0.58 ± 0.09	0.59 ± 0.08	0.56 ± 0.09
NOE and van der Waals target function (Å^2)	0.33 ± 0.05	0.75 ± 0.12	0.60 ± 0.11	0.91 ± 0.13
total target function (Å^2)	0.33 ± 0.05	0.80 ± 0.12	0.90 ± 0.12	1.17 ± 0.18
av violation per NOE constraint (Å)	0.0017 ± 0.0002	0.0028 ± 0.0004	0.0026 ± 0.0004	0.0033 ± 0.0005
av no. of violations >0.05 Å per structure	14 ± 4	25 ± 5	23 ± 6	30 ± 5
av no. of violations >0.2 Å per structure	0 ± 1	1 ± 1	1 ± 1	1 ± 1
largest residual NOE violation (Å)[c]	0.29	0.43	0.35	0.50
av deviation per pcs constraint (ppm)[d]	0.3 ± 1.1	0.029 ± 0.005	0.3 ± 1.6	0.04 ± 0.02
av no. of pcs violations	33.1 ± 4.7	13.7 ± 3.3	30.8 ± 3.8	15.8 ± 3.0
av deviation of Δrdc values (Hz)[d]	0.17 ± 0.12	0.19 ± 0.14	0.028 ± 0.004	0.021 ± 0.002
av no. of Δrdc violations	50.4 ± 2.3	53.9 ± 2.3	36.8 ± 4.1	34.1 ± 3.8

[a] All values are averaged over the best 20 conformers, unless otherwise indicated. [b] These values have been recalculated by using the present DYANA structures, as discussed in the experimental part, for comparison purposes. [c] Largest violation among all 20 conformers. [d] Average deviation between experimental and calculated values.

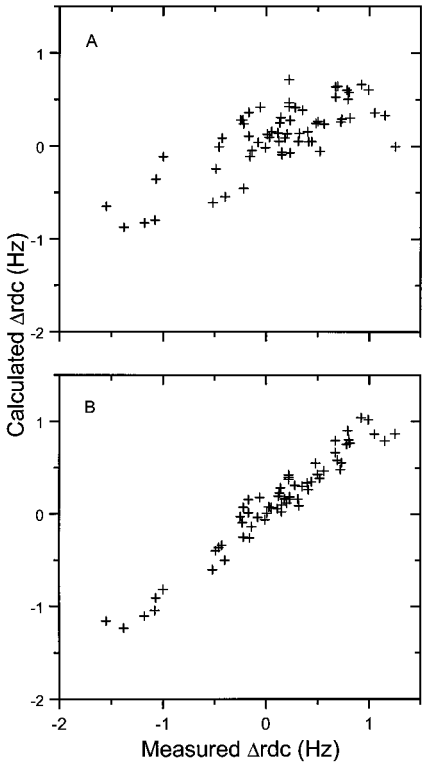

Figure 1. Observed versus calculated Δrdc values for the previously determined family of conformers of oxidized cyt b_5[24] (A) and for the refined family (B).

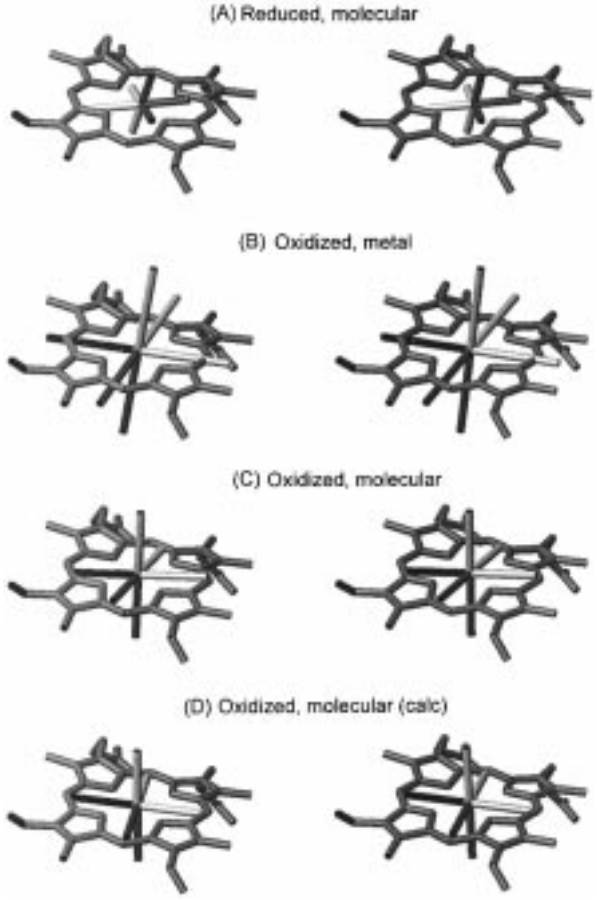

Figure 2. Comparison of the χ^{dia} tensor of reduced cyt b_5 (A), the χ^{para} (B) and the χ^{mol} (C) tensors of oxidized cyt b_5, and the calculated χ^{mol} tensor of oxidized cyt b_5 as the tensorial sum of χ^{dia} and χ^{para} (D). The length of the axes reflects the relative values of $\Delta\chi_{ax}$. The tonality of the tensor axes in (A) is inverted to show pictorially that $\Delta\chi_{ax}$ has opposite sign with respect to the other tensors.

2 and 3). The mean deviation between calculated and experimental Δrdc values is much smaller than that for the initial families obtained without the new constraints (Tables 2 and 3 and Figure 1), indicating that there has been a reorganization of the protein structure to better satisfy the Δrdc constraints.

The final χ^{mol} tensor parameters for the reduced and oxidized species are reported in Table 1, together with the values relative to the χ^{para} tensor of the metal ion, obtained from the fitting of pcs. Figure 2 shows a comparison of the three tensors. Note that the tensor parameters in Table 1 are consistent with the solution structures. In previous works,[14,39−45] except the most recent ones from our laboratory,[24,28,46−48] the χ^{para} tensor parameters have been obtained from NMR data and X-ray coordinates, which are not necessarily equal to the solution coordinates.

(38) Wüthrich, K. *NMR of Proteins and Nucleic Acids*; Wiley: New York, 1986.
(39) Williams, G.; Clayden, N. J.; Moore, G. R.; Williams, R. J. P. *J. Mol. Biol.* **1985**, *183*, 447−460.
(40) Feng, Y. Q.; Roder, H.; Englander, S. W. *Biochemistry* **1990**, *29*, 3494−3504.
(41) Gao, Y.; Boyd, J.; Pielak, G. J.; Williams, R. J. P. *Biochemistry* **1991**, *30*, 1928−1934.
(42) Emerson, S. D.; La Mar, G. N. *Biochemistry* **1990**, *29*, 1556−1566.
(43) Rajarathnam, K.; La Mar, G. N.; Chiu, M. L.; Sligar, S. G. *J. Am. Chem. Soc.* **1992**, *114*, 9048−9058.
(44) La Mar, G. N.; Chen, Z. G.; Vyas, K.; McPherson, A. D. *J. Am. Chem. Soc.* **1995**, *117*, 411−419.
(45) Tolman, J. R.; Flanagan, J. M.; Kennedy, M. A.; Prestegard, J. H. *Nature Struct. Biol.* **1997**, *4*, 292−297.

The backbone RMSD values of the family of conformers of oxidized cyt b_5 (with NOE and pcs constraints) with and without Δrdc constraints are essentially the same (0.56 ± 0.09 and 0.58 ± 0.11 Å, respectively), whereas the average NOE and van der Waals target function is slightly higher for the former family (0.75 ± 0.12 and 0.91 ± 0.13 Å^2, respectively). Also in the case of reduced cyt b_5, the backbone RMSD value obtained after introduction of the new constraints is close to that previously obtained (0.74 ± 0.14 and 0.76 ± 0.11 Å, respectively), whereas the target function values in the two cases are very similar (0.95 ± 0.18 and 0.94 ± 0.20 Å^2, respectively). For both oxidized and reduced cyt b_5, the overall folding obtained with Δrdc constraints is essentially identical to that obtained without such constraints. The backbone RMSD between the two mean structures is 0.4 Å, i.e., well below the RMSD within each family. This means that the two sets of constraints are consistent (see also below) and that when there are few NOEs, but a reasonable number of ^{15}N−^{1}H and ^{13}C−^{1}H Δrdc constraints are available, the Δrdc constraints may be very precious. Even in the present example, the new family, which satisfies both sets of constraints, can be considered more accurate than the family obtained without the Δrdc constraints (which was not in agreement with the experimental Δrdc values).

Discussion

Comparison between the Structures of Cytochrome b_5 Obtained with and without Δrdc Constraints. The effect of the introduction of a new class of structural constraints in a structure calculation protocol must be assessed with respect to two points: (i) effect of the new constraints on the accuracy and precision of the structure and (ii) consistency with the old constraints. For reduced cyt b_5, the family of conformers obtained with NOE and Δrdc constraints must thus be compared with that obtained only with NOE constraints (Table 2). For oxidized cyt b_5, there are three different classes of constraints: NOE, pcs, and Δrdc. To dissect the contribution to the target function and to understand the consistency among these three groups, it is necessary to compare the results of four structure calculations: with NOE alone, with NOE and pcs, with NOE and Δrdc, and with NOE, pcs, and Δrdc (Table 3). The calculations were performed with strictly the same protocol.

In the case of reduced cyt b_5 the RMSD of the structure, which is a measure of its precision, decreased slightly but not significantly, upon introduction of the new constraints, and the target function of NOE and van der Waals violations is minimally affected. All the parameters quantifying the agreement between the obtained family of conformers and the NOE constraints are essentially unchanged (last four entries in Table 2). The family of conformers obtained only with NOE was already in good agreement with the experimental Δrdc values, displaying a mean error of 0.07 Hz. In the family calculated using the Δrdc as constraints, the error dropped to 0.03 Hz.

For oxidized cyt b_5, again no significant changes in the precision of the structure with respect to that obtained just with NOE constraints is observed when either pcs or Δrdc constraints were introduced (Table 3). A slight increase of NOE violations is observed in both cases. The combined use of the three groups of constraints does not produce a significant decrease of the backbone RMSD. A further slight increase of NOE violations is observed. However, it should be observed that this small increase of the NOE violations is more than counterbalanced by a nearly 10-fold decrease in the deviation between experimental and calculated pcs and Δrdc values, which is obtained upon introduction of these constraints. It can be also noted that when pcs and Δrdc constraints are used together (and together with NOE), the average errors obtained on these constraints are not significantly higher than those obtained when each constraint is used individually. In other words, the error on the pcs values reported in column 2 of Table 3 is not significantly different from that reported in column 4, and the same holds for the errors on the Δrdc values reported in columns 3 and 4. This indicates that these two sets of nonstandard constraints are fully compatible with one another and that they contribute to increase the accuracy of the structure even if within the same RMSD values.

Comparison of the χ^{mol} Tensors of Oxidized and Reduced Cytochrome b_5 with the χ^{para} Tensor of the Metal Ion. Bax and co-workers had previously demonstrated that for the diamagnetic ubiquitin molecule there is reasonable agreement between the tensor parameters obtained by fitting the experimental dipolar couplings to the static crystal structure and the tensor parameters calculated by summing up all the magnetic susceptibility tensors of the individual amino acids (within 15% for the axial component, the rhombic component being much smaller and affected by a large error).[14] On the other hand, in the paramagnetic complex of metmyoglobin−cyanide, the χ^{mol} tensor parameters computed from the experimental Δrdc using the crystal structure differs by ∼30% for the axial component from that estimated by summing up the χ^{para} tensor obtained from pseudocontact shifts[42] (which is due to the paramagnetic susceptibility and is larger than the overall tensor) and all the diamagnetic contributions to the magnetic susceptibility (i.e., those of the heme moiety [4] and of the polypeptide chain[49−51]). To rationalize this discrepancy, the existence of slow large-scale collective motions in myoglobin was postulated,[45] an interpretation criticized by other authors.[52]

In light of what outlined above, it is interesting to compare the final χ^{mol} tensor parameters obtained for oxidized cyt b_5 (Figure 2C) to the χ^{para} tensor parameters (Figure 2B). First, let us consider what the χ^{mol} tensor of the oxidized species should be. The most relevant contributions to the χ^{mol} in paramagnetic heme-containing systems are those due to the metal ion and the porphyrin moiety. These are of the same order of magnitude. Both are roughly 1 order of magnitude larger than the contributions due to the side chains of the various aromatic groups,[49] and 2 orders of magnitude larger than the contribution due to the magnetic anisotropy of the peptide bonds.[50,51] Thus, to a first approximation, the molecular tensor can be calculated by summing the two above-mentioned contributions.

From inspection of Table 1 and Figure 2, it can be immediately observed that the χ^{para} tensor and the χ^{mol} tensor of oxidized cytochrome b_5 have, within experimental error, the same orientation with respect to the heme moiety, and the same rhombic anisotropy. Instead, the axial anisotropy of χ^{mol} is somewhat smaller than that of χ^{para}. This is in complete agreement with that expected from the available data on

(46) Banci, L.; Bertini, I.; Bren, K. L.; Cremonini, M. A.; Gray, H. B.; Luchinat, C.; Turano, P. *JBIC, J. Biol. Inorg. Chem.* **1996**, *1*, 117−126.
(47) Banci, L.; Bertini, I.; Bren, K. L.; Gray, H. B.; Sompornpisut, P.; Turano, P. *Biochemistry* **1997**, *36*, 8992−9001.
(48) Banci, L.; Bertini, I.; De la Rosa, M. A.; Koulougliotis, D.; Navarro, J. A.; Walter, O. *Biochemistry* **1998**, *37*, 4831−4843.
(49) Giessner-Prettre, C.; Pullman, B. *Q. Rev. Biophys.* **1987**, *20*, 113−172.
(50) Tigelaar, H. L.; Flygare, W. H. *J. Am. Chem. Soc.* **1972**, *94*, 343−346.
(51) Williamson, M. P.; Asakura, T. *J. Magn. Reson. Ser. B* **1993**, *101*, 63−71.
(52) Bax, A.; Tjandra, N. *Nature Struct. Biol.* **1997**, *4*, 254−256.

magnetic susceptibility anisotropy of porphyrins.[4] Indeed, the magnetic susceptibility tensor for the heme porphyrin is expected to be essentially axial (i.e., with near-zero rhombic anisotropy), with its principal axis orthogonal to the heme plane, and with a negative $\Delta\chi_{ax}$ value. The difference in $\Delta\chi_{ax}$ between the χ^{para} and the χ^{mol} tensors is $(-0.6 \pm 0.2) \times 10^{-32}$ m^3 (Note that this difference is already qualitatively meaningful because the two tensors are essentially collinear. The results of the proper tensorial difference are discussed below.)

The parameters of the molecular magnetic susceptibility tensor (χ^{dia}) obtained for reduced cyt b_5 are also reported in Table 1. $\Delta\chi_{ax}$ is equal to $(-0.8 \pm 0.1 \times 10^{-32}$ m^3, whereas the rhombic anisotropy is not significantly different from zero (Figure 2A). The $\Delta\chi_{ax}$ values reported in the literature for other porphyrins are in the range $(-1.0$ to $-1.3) \times 10^{-32}$ m^3,[4] which is in reasonable agreement with the present result. The deviation of the *z* axis of the χ^{dia} tensor from the normal to the heme plane is probably due to the relatively large error in measuring the Δrdc values for reduced cyt b_5, together with the large uncertainty of the parameters at values of θ (eq 2) close to zero. Indeed, the increase of the average deviations of the calculated Δrdc from the experimental values obtained when this angle is changed within $\pm 15°$ is modest and below the error on the experimental Δrdc values.

The results obtained for the χ^{mol} tensor of oxidized cyt b_5 are in good agreement with that expected from the tensorial sum of the χ^{dia} tensor of the reduced species and the χ^{para} tensor of the metal (see Table 1 and Figure 2C,D). The fact that these two *independent* estimates of the χ^{mol} tensor parameters of oxidized cyt b_5 agree further demonstrates that the methods used for the determination of the molecular magnetic susceptibility tensor described in this article and of the χ^{para} tensor of the metal ion[20,24,27,28] are adequately accurate and provide reliable results.

Finally, we would like to stress that we have been able to measure significant rhombicity of the susceptibility tensor ($\chi_{rh} \sim {}^1/_2\chi_{ax}$ for the oxidized protein) and that a sizable rhombicity allows the determination not only of the orientation of each NH vector with respect to the χ_{zz} axis (θ angle in eq 2) but also of its projection in the *xy* plane (ϕ angle in eq 2). This feature permits the full exploitation of Δrdc's as structural constraints.

Conclusions

In the present study, the solution structures of oxidized and reduced cyt b_5 have been refined by including Δrdc's couplings in structure calculations. For this purpose, a new routine has been implemented in the PSEUDYANA module[25] of the program DYANA.[23] This is the first report of the use of Δrdc constraints for solution structure refinement of a paramagnetic protein.

The structure has been calculated with rdc constraints and both NOEs and NOE + pcs constraints. The results show that there is good agreement between the three sets of constraints. These calculations provide as output the χ^{mol} tensor parameters, making the structure consistent with the Δrdc values, and the χ^{para} tensor, making the structure consistent with the pcs. As a result, we have obtained the χ^{mol} tensor parameters of the paramagnetic oxidized and the χ^{dia} tensor parameters of the diamagnetic reduced proteins, together with the χ^{para} contribution which was already available from the pcs.[24]

The χ^{dia} tensor parameters of the reduced species are in good agreement with previously reported data for free porphyrins in solution.[4] This shows that the contribution of the amino acidic part of the system is at least 1 order of magnitude smaller than that of the diamagnetic heme moiety, as expected. The χ^{mol} tensor parameters of the oxidized protein are in good agreement with that expected from those of the χ^{dia} tensor of the reduced species and of the χ^{para} tensor of the metal ion.[24] The present results are thus important also with respect to the debate on the relative weight of paramagnetic and diamagnetic contributions and on its general implications for the presence of large-scale motions in proteins.[45,52]

In summary, the present work provides a picture of the advantages of introducing metal ions with large $\Delta\chi_{ax}^{para}$ and $\Delta\chi_{rh}^{para}$ into macromolecules, which may be suggested as a new technique to gain access to further structural information both through partial orientation effects and through paramagnetically induced shifts. These new constraints, which are long range in nature, are particularly precious when the classical constraints are relatively few.

Acknowledgment. We thank Dr. S. G. Sligar for generously providing the gene encoding the soluble fragment of rat cyt b_5, Dr. Christine Cavazza for the culture and purification of ^{15}N-enriched cyt b_5, and Dr. M. A. Cremonini for helpful discussions on the implementation of the Δrdc constraints in DYANA. J.G.H. acknowledges EU for a postdoctoral fellowship. The EU financial support (Contract ERBFMGECT950033) is gratefully acknowledged. This research has been partly supported (40%) by MURST.

Supporting Information Available: Experimental Δrdc values and pairwise differences between the two sets of experiments at 18.8 and 11.8 T field for oxidized cytochrome b_5 and at 11.8 T for reduced cytochrome b_5 (4 pages, print/PDF). See any current masthead page for ordering and Internet access instructions. See any current masthead page for ordering information and Web access instructions.

JA981791W